$\bar{p}$ PRODUCTION AND COLLECTION

Eifionydd Jones
CERN, Geneva, Switzerland

1. INTRODUCTION

The CERN Proton Synchrotron (CPS) conveniently provides more than 10^{13} protons at 26 GeV/c every 2.4 seconds. These protons arrive in bunches at the $\bar{p}$ target; there are five bunches inside a total pulse time equal to 0.4 μs, just less than the revolution period of a 3.5 GeV/c $\bar{p}$ on the AA injection orbit. The proton beam has a momentum spread $\Delta p/p$ of about $\pm 3 \times 10^{-3}$ and a transverse emittance (E) in both planes of a few $\pi \times 10^{-6}$ m.rad. The target diameter is 3 mm and 95% of all the protons are focused to a minimum beam radius of 1.2 mm inside the target. The target length is 11 cm and the beam radius changes by about 0.2 mm over this distance. The β value, defined by $2\sigma_{rms} = \sqrt{\beta E/\pi}$ (E = transverse emittance, β = Twiss parameter), is between 0.4 to 0.5 m with σ_{rms} one standard deviation of the gaussian assumed to represent the proton beam transverse density distribution. In the following, whenever computer modelling is mentioned such gaussian beams are always used. However, the looser term "beam radius" is also used and this is taken to be $2\sigma_{rms}$ so that 95% of the beam is to be found inside its so-called radius.

Antiprotons emerge from the target, along with many other fundamental particles, and are focused by a cylindrical lens, called a magnetic horn, into the beam transport system. The latter consists of an arrangement of strong focusing quadrupoles and a spectrometer magnet* as shown in Fig. 1. The transport system selects negatively charged particles of nominally 3.5 GeV/c with a momentum spread of 1.5% and matches them into the transverse acceptance of the AA. The AA is designed to have a nominal transverse acceptance of 100 $\pi \times 10^{-6}$ m.rad in both planes. The unstable particles, mostly π^- which have also found their way onto the AA injection orbits, decay away. The electrons injected at the same time lose energy by synchrotron radiation, spiral towards the central orbits and are lost on the various shutters belonging to injection and cooling devices. The information from the lost electrons is used to adjust the injection parameters so as to minimize coherent oscillations of the $\bar{p}$'s[1].

*(orig./HSI)

The performance of the $\bar{p}$-production system is measured in terms of the $\bar{p}$ yield Y, where

$$Y = \frac{\text{no. of } \bar{p}\text{'s left circulating in the AA}}{\text{no. of p's falling on the target}}$$

Typically $Y \simeq 6 \times 10^{-7}$.

The reasons for this choice of $\bar{p}$-production system are outlined below.

2. THE $\bar{p}$-YIELD IS A FUNCTION OF θ^2 AND Δp AND THE PROPERTIES OF THE TARGET

The $\bar{p}$-production cross-section was dealt with in the lecture by J.V. Allaby. The cross-section reaches a flattish maximum for $\bar{p}$'s produced by a 26 GeV/c protons around 4 GeV/c. The geometry and straight-section space needed for the AA lattice is such that the bending magnets have a magnetic field of 1.8 T (about maximum for iron cores) and can handle momenta of at most 3.5 GeV/c. Hence the choice of nominal momentum. The longitudinal or momentum acceptance of 1.5% is dictated by the capabilities of the precooling system, and the transver-

se acceptance of 100π mm.mrad by economic considerations related to the size of the apertures of quadrupoles and bending magnets. The largest bending magnets weigh 60 tons.

Figure 2 compiled by C.D. Johnson[2] from the literature on $\bar{p}$ production cross-sections illustrates the measured yields per interacting proton of 24 GeV/c for $\bar{p}$'s of 4 GeV/c and various target materials. The yield peaks at forward production angles and appears to vary exponentially with production angle at least up to angles of 100 mradians (see J.V. Allaby).

Thus the yield per interacting proton may be roughly estimated for a copper target as:

$$N_{\bar{p}} = 0.009 \ \Delta p \ (\text{GeV/c}) \ \Delta\Omega \ (\text{steradian})$$

for $\bar{p}$'s in the range of production angles around zero degrees.

For the AA the momentum bite $\Delta p = 0.015 \times 3.57$ (GeV/c) and $\Delta\Omega = \pi\theta_{max}^2$ with θ_{max} the maximum angle that can be accepted by the beam transport system and matched into the AA acceptance of $100\pi \times 10^{-6}$ m.rad.

Some of these $\bar{p}$'s will be reabsorbed by the target nucleons and most of them will be coulomb scattered by the electric charge of the target nucleons. However, since most particles are to be found at the largest angles it turns out that multiple coulomb scattering is a negligibly small effect for the long thin targets normally used. As for reabsorption, those $\bar{p}$'s produced at smaller angles spend a longer time traversing the target than those at larger angles, so that the reduction in yield with production angle is largely compensated for by reabsorption effects. Hence we can write with good accuracy for a copper target 3 mm in diameter and 110 mm long:

$$N_{\bar{p}} = 0.009 \times 0.015 \times 3.57 \times \pi \times \theta_{max}^2$$

$$= 1.5 \times 10^{-3} \times \theta_{max}^2 \text{ per interacting proton.}$$

If N_{p_0} is the number of protons entering a target of length L, the number N_p which will interact with the target nucleons is simply:

$$\frac{N_p}{N_{p_0}} = \left[1 - \text{EXP} \left(- \frac{L}{\lambda_{abs}} \right) \right]$$

where λ_{abs} is the absorption length for 26 GeV/c protons in the target material. For copper λ_{abs} = 140 mm, so that in a target length of 110 mm only about two thirds of the protons are "interacting" ! Thus the yield Y quoted above for the AA is essentially:

$$Y = \frac{2N_{\bar{p}}}{3} \simeq 10^{-3}\theta_{max}^2 \ .$$

This implies that since we measure Y to be 6×10^{-7} the maximum angles accepted by the AA do not exceed about 50 mradians.

However, this simple approach is only illustrative and serves only to demonstrate the physics behind the choices made for the AA $\bar{p}$-production system. Some of the details of why we choose for example copper and not beryllium or even tungsten are examined below.

3. FOCUSING SYSTEM FOR $\bar{p}$ COLLECTION

The $\bar{p}$-collection system consists of a number of electromagnetic lenses along with a bending magnet for momentum selection. The longitudinal acceptance of 1.5% in $\Delta p/p$ for the AA is not unusual for a beam transport system consisting mainly of strong focusing quadrupoles.

However, in order to get a good yield of $\bar{p}$'s, we have seen above that we must try to capture particles having production angles of at least 50 mrad and if possible even upt to 100 mrad. Every doubling of the angle results in quadrupling the yield, at least in theory.

A well designed quadrupole, iron cored and powered by copper windings, can have a magnetic field gradient g of:

$$g \simeq 10 \text{ Wb m}^{-3} \text{ (T.m}^{-1}\text{)}$$

and it will have a strength (or inverse "focal length f" in thin lens approximation) for a nominal length ℓ.

$$\frac{1}{f} = k\ell \quad ; \quad k = \frac{e}{p} g \quad ,$$

or

$$\frac{1}{f} \simeq \frac{1}{3\gamma\beta} g \text{ (Wb m}^{-3}\text{)} \ell(\text{m}) \quad [\text{m}^{-1}]$$

with γ and β the usual relativistic parameters.

The $\bar{p}$'s injected into the AA have $3\gamma\beta \simeq 10$, so that a focal length of a metre with g = 10 T.m^{-1}, would seem entirely feasible for a lens around one metre long.

Thus, from the simplest considerations, such a lens placed with its centre one metre away from the target would need to have a half-aperture R where $R = f\theta$ (and θ = production angle) of between 50 to 100 mm in the focusing plane and about twice this amount in its defocusing plane. Obviously, the next quadrupole downstream has alternate focusing planes, but nevertheless would now need to be able to handle angles between 100 and 200 mrad in at least one plane.

Hence, apertures become embarrassingly large, the pole tips will saturate, and we really need to introduce a cylindrical lens immediately after the target, focusing in both (or all) planes at once, which reduces the angles to be handled by the normal quadrupoles by at least a factor of ten.

3.1 Cylindrical Magnetic Lenses

K.G. Steffen in the first five pages of his book "High Energy Beam Optics" describes two conceptually simple cylindrical magnetic lenses.

The first he calls the "wire lens" in which a uniform current density j_0 is passed axially along a cylindrical conductor such that the magnetic gradient inside it is constant and given by:

$$g = \frac{\mu_0 \mu j_0}{2} .$$

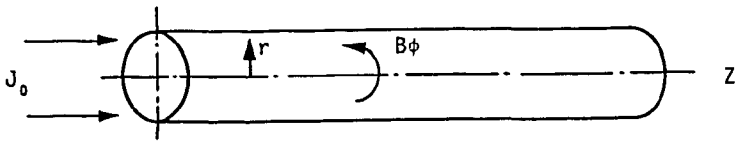

The polar magnetic field is given as a function of the radius r:

$$B\phi = gr \ .$$

The second lens Steffen describes is the "parabolic current sheet lens" in which current is passed along a conducting sheet of parabolic shape and cylindrical symmetry:

Thus, $B\phi \propto 1/r$ and for $\ell \propto r^2$ (parabola) the lens gradient $g \propto 1/r^2$ and its strength $\propto g\ell$ is independent of the radius. This is then a linear cylindrical focusing device. It appears to have been first described by H.G. Hereward and M. Hine. In the USSR it is called the "Ha" lens.

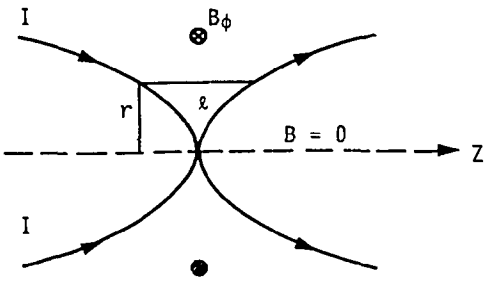

Today, the best known "wire lenses" are the so-called lithium lenses of Novosibirsk and FNAL, in which the wire conductor is a cylindrical rod of lithium contained inside a titanium and steel shell. These lenses in order to compete with a strong focusing quadrupole capable of focusing a 3.5 GeV/c beam inside a length of one metre have to achieve gradients of 10 Wb m^{-3} or current densities of 16 $A.mm^{-2}$.

Quadrupoles can have "comfortable" full apertures of 200 mm so that a wire lens of the same scale would need a current of 500 kA. However, optimum designs for wire lenses do not need such large apertures, it suffices to say that the largest lithium lenses being built today have full apertures of more nearly 20 mm and are about 100 mm in length. They do, however, support currents of up to 500 kA but not without considerable technological skill in their construction.

Similarly, the parabolic current sheet lens, to compete, needs 5000 kA pulsed along its conducting walls. Another tehnological nightmare for both the electrical and mechanical designer.

However, in the AA, we use a development of this second type of lens, due to S. van der Meer, called the magnetic horn. This was first described in CERN yellow report [3] in 1962 and treated again by E. Regenstreif [4] in 1964.

Full details of the theory are given in the above references.

3.2 The Magnetic Horn

The horn is a current sheet lens shaped thus:

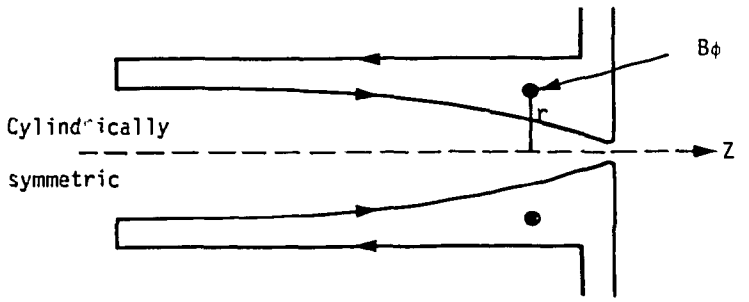

Again $B\phi \propto 1/r$ but the exact profile of the inner conductor is chosen such that it can focus large angle particles from the target. It has a reasonably extended depth of focus and can shape the beam emittance at its exit into a rectangular (or elliptical) area having, for $100\pi \times 10^{-6}$ m.rad, dimensions approaching a 20 mm beam radius with angles of up to 5 mrad.

It is highly non-linear and concentrates upon focusing the larger production angles (where most of the $\bar{p}$'s are to be found) while maintaining a depth of focus equal to an appreciable fraction of the target length.

The detailed design is carried out entirely by means of a computer model based upon the $\bar{p}$ production cross-section data for particular target materials. The equivalent depth of focus amounts to less than 10 cm so that target materials have to be chosen such that the proton absorption length λ_{abs} is of this order. Hence our choice of the somewhat heavier materials. The initial choice was tungsten but measurements carried out at the AA showed that copper was slightly better.

The final profile of the inner conductor is arrived at by tracing many particles through the magnetic fields produced by a first-guess-profile and subsequently altering interactively the parameters in the computer model until the scatter graphs of particles in the phase space at the exit of the horn gives the largest number of particles emerging into $100\pi \times 10^{-6}$ m.rad.

Figure 3 shows the scatter-graphs of population density at the centre of the AA target and Fig. 4 the same graphs at the exit of the target-horn arrangement presently used in the AA.

These calculations were carried out by T.R. Sherwood using Monte-Carlo techniques and follow closely those of S. van der Meer[3].

Example: Design a "first-guess" horn profile.

In order to get a first-guess at the profile of the inner conductor of a horn, for data input to the computer model, the following approach may be used.

Calculate the trajectories of a charged particle moving in a cylindrically symmetric field with strength inversely proportional to a radius.

In cylindrical polar coordinates:

$\bar{B}\phi = \bar{a}\phi(\mu\mu_0 I/2\pi r)$, the field outside the inner profile produced by a current I.

$= 0$, inside the profile.

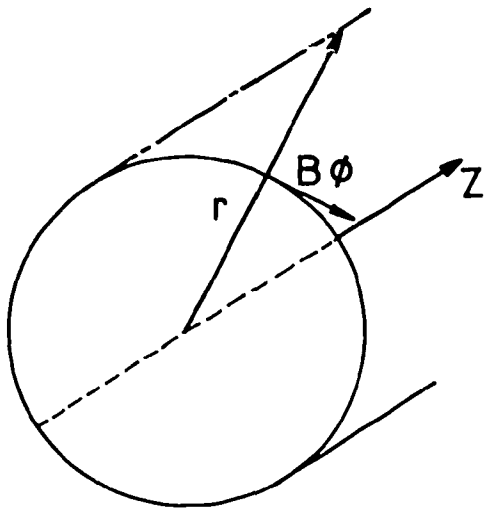

The equation of motion (derived from the Lorenz equation) is:

$$\frac{d^2r}{dz^2} + \frac{A}{r}\left[1 + \left(\frac{dr}{dz}\right)^2\right] = 0 . \qquad (1)$$

Assume (for simplicity), no skew rays i.e. $d\phi/dt = 0$ and that $dr/dt \ll dz/dt = v_z$ such that $d/dt = v_z(d/dz)$.

Further assume no coulomb scattering in the aluminium shell carrying the current.

In equation (1)

$$A = \frac{e}{p}\frac{\mu\mu_0}{2\pi} \cdot I \; ; \quad p = mv_z .$$

Finally, we can assume that $dr/dz \ll 1$ since the production angles to be captured are very likely not greater than 100 mrad i.e. $(dr/dz)^2 < 0.01$.

This means equation (1) reduces to:

$$rr'' = -A , \qquad (2)$$

$$r' = \frac{dr}{dz} ; \quad r'' = \frac{d^2r}{dz^2} .$$

Consider the following geometry wherein a particle leaving the target at angle θ_1 arrives at the inner conductor at r = R1 and leaves the exit face of the horn at r = Rm on a trajectory parallel to the z-axis.

Equation (2), with these initial conditions, can be integrated to give:

$$r' = [\theta_1^2 - 2A \cdot \mathrm{LOG}(r/R_1)]^{1/2}$$

and since the trajectory is parallel to the z-axis upon leaving the end face,

$$r' = 0 \quad \text{at} \quad r = Rm ,$$

so that

$$Rm = R_{max} = R1 \; \mathrm{EXP}(\theta_1^2/2A) . \qquad (3)$$

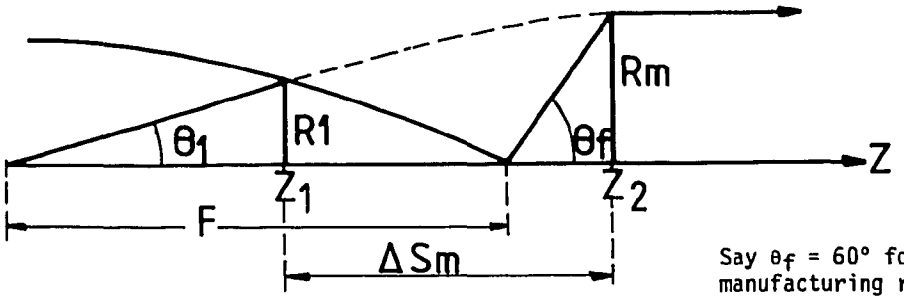

Say $\theta_f = 60°$ for manufacturing reasons.

From (3):

$$\Delta S_m = \int_{z_1}^{z_2} dz = \int_{R1}^{Rm} \frac{dr}{[\theta_1^2 - 2A \cdot LOG(r/R1)]^{1/2}} \quad . \tag{4}$$

Equation (4) can be re-written in terms of error integrals:

$$\Delta S_m = \frac{R1}{A^{1/2}} EXP\left(\frac{\theta_1^2}{2A}\right) \int_0^{\theta_1/A^{1/2}} e^{-t^2/2}\, dt ,$$

or

$$\Delta S_m = \frac{R_m}{A^{1/2}} Int(\theta_1) ,$$

with

$$R_m = R1\ EXP(\theta_1^2/2A) ,$$

and

$$Int(\theta_1) = \int_0^{\theta_1/A^{1/2}} e^{-t^2/2}\, dt \quad .$$

The profile R1 versus θ_1 can then be calculated from (using the nomenclature of the diagram):

$$R1 = \frac{F \tan\theta_1}{\left[1 + \tan\theta_1 \left(\frac{Int(\theta_1)}{A^{1/2}} - \frac{1}{\tan\theta_f}\right) EXP\left(\frac{\theta_1^2}{2A}\right)\right]} \quad .$$

This profile is then fed into the computer model and particles are traced through the now known magnetic field. At the exit of the horn, a count is made of no. of particles to be

found inside the 100π transverse acceptance of the AA. This particle count is maximized by varying the obvious parameters such as the total current I, the target material, and its dimensions and horn-target distances.

4. TECHNOLOGY AND ENGINEERING

In the above nothing has been said about the manufacturing or operational problems relating to either targets or horns. In the following an attempt is made to remedy this. The work described below was carried out by G. Lebée[5] on the horn and P Sievers et al.[6] on the target. The installation of the devices was engineered by B. Szeless with a lot of help from the CERN technical and safety groups and a lot of interference from myself.

4.1 The Production Target

The target should be made of a material which has a relatively short proton absorption length, λ_{abs}, in order to help the focusing device placed after it. The parameters of the focusing systems are such that a target diameter of 3 mm and a length of the order of 10 cm should be aimed at. Examination of the literature indicates that the choice of material lies between tungsten λ_{abs} = 10 cm and lead λ_{abs} = 17 cm, with in between copper λ_{abs} = 14 cm. Copper has the advantage over the other two materials from the point of view of the radiation length λ_R influencing coulomb scattering; λ_R being two to three times larger for copper than, respectively, lead and tungsten.

The first targets used were made of tungsten 11 cm long and 3 mm in diameter. They had to withstand 10^{13} protons per pulse at a momentum of 26 GeV/c. The duration of each proton burst is 0.4 s and the repetition time is 2.4 s. 67% of the incident protons will be "absorbed" in the material. The energy of the incident proton beam is 41 kJ per pulse, of which about 2.6 kJ are deposited in the target. This corresponds to an average power dissipation of 1.1 kW at full repetition rate.

These estimates of power dissipation come from calculations of the energy deposited by the incident protons and the nuclear-meson cascade induced in the target. They have been carried out with the Monte-Carlo cascade programme ZYLKAZ developed by J. Ranft[7]. The calculations estimate that the adiabatic temperature rise along the axis of the target, at each pulse, approaches 1350°C for tungsten and 400°C for copper. After a few milliseconds the temperature drops. These values indicate that thermal shock may well fracture the target material, and in order to avoid its disintegration through oxidation or evaporation, the container must be capable of containing any targets that fragment and must stand these elevated temperatures. The container should also be of a low density material so that $\bar{p}$'s emerging from the target are not re-absorbed. Graphite was selected as the material for the target container since it has all of the required properties. It has excellent mechanical and thermal properties at elevated temperatures of up to 3000°C and can easily withstand the heating of a beam misteered onto it.

The tungsten target consists of a string of 11 cylinders of 3 mm diameter and 10 mm in length, fitted into a hole drilled along the core of a graphite cylinder having an outside diameter of 30 mm. At either end graphite plugs are screwed into the graphite container to seal off the target. To avoid oxidation, the tungsten-graphite assembly is further enclosed in a finned aluminium cylinder which is sealed-off with titanium windows at either end.

Figure 5 shows an overall view of the target assembly. The fins are to help in air cooling. Such targets have withstood over a 1000 hours in continuous operation and do not appear to sustain any such permanent damage that might reduce the $\bar{p}$-yield.

Copper targets are made in the same manner, simply replacing the tungsten cylinders by copper rods. A copper target consisting of one single rod 11 cm long has also been tested in a beam of 2×10^{13} protons per pulse, every 2.4 s for a few hours, in an attempt to destroy it. However, it withstood the test and the outside temperature of the aluminium container never exceeded 50°C in the presence of the standard air cooling system having an air speed around the fins of 10 $m.s^{-1}$.

With a tungsten target the aluminium container heats up to around 100°C with a beam of 10^{13} protons per 2.4 s. As a result of the overall cooling the average surface temperature of the tungsten rod is estimated to be at most 800°C. Therefore the temperature along the tungsten core will rise to at most 2150°C after each proton pulse in continuous operation. That of a copper core will rise to 800°C from an average value of 400°C.

In practice copper targets give the best $\bar{p}$ yield and would seem to suffer less from the thermal treatment produced by the beam. They have operated for many thousands of hours without failure.

4.2 The Horn

Figure 6 shows the magnetic horn assembly. It is seen to be about 40 mm in diameter at the exit face and about 40 cm overall length. The inner cylindrical shell is of an aluminium alloy (Anticorodal A112) machined from a solid block. The inner shell is 1 mm thick and hence absorbs only about 10% of the $\bar{p}$'s. The current pulse needed is 160 kA in the form of a half-sine wave ~16 μs long. Current is fed into the horn via a sandwich line from a capacitor bank (ten parallel units of 20 μF) charged to 4.5 kV. The parasitic inductance of one unit is 400 nH. The system is crowbarred into a damping resistance of 130 mΩ. All the switching is carried out by ignitrons.

The pressure exerted by the magnetic field on the inner cylindricyl shell is 65 $kg.cm^{-2}$ (65×10^5 $N.m^{-2}$) at the largest diameter. The pressure is proportional to I^2/r^2 with r the cylinder radius, hence near the exit membrane where r is 4.5 mm, the pressure gets up to a maximum of 425 $kg.cm^{-2}$. These forces squeeze the horn and pushes the exit membrane outwards at each pulse.

The horn shell and membrane have to withstand these pressures for over a million cycles. The critical pressures for buckling in cylinders is proportional to r^{-3} so that the largest diameters are most critical. The static critical buckling pressure for the AA horn is 120 $kg.cm^{-2}$ for a 1 mm thick shell. The stresses in the exit membrane are reduced by sloping it away from the horn shell.

However, because the pressure is applied in the form of a very short impulse, the material does not have the time to move and does not collapse - at least if it is thick enough. The final thickness arrived at, of 1 mm, was after many prototype tests with shells of 0.5 mm, 0.7 mm and 1 mm thick. During these tests the 0.5 to 0.7 mm thick shells ruptured after 0.5×10^6 discharges. However, the 1 mm thick horn presently in use has so far survived for over 10^6 discharges of 160 kA every 2.4 s. An earlier horn of identical design was destroyed

by the beam during attempts to steer the protons onto the target. The only other problem has been due to electrical breakdown of a connector attached to the sandwich line for monitoring purposes.

4.3 The Target-Horn Assembly

The target and horn are mounted on vee-blocks. These vee-blocks are carefully pre-aligned on a marble block. Figure 7 shows a side view of the assembly. The block itself is equipped with various ducts for the air cooling system and a quick connect device consisting of a lever and spring arrangement holds the horn and sandwich line in place. The target sits on its vee-block held in place by gravity only, and in fact, due to the considerable blow delivered by the proton beam, rotates slowly clockwise !

The marble block has three feet in the form of three open cones which fit over three studs previously aligned in the target bunker.

All of these materials and methods are necessary because in operation just one day after the beam has ceased to hit the target, the radioactivity is such that the dose-rates close to the target are a few hundreds of rem per hour. The target area has been designed such as to shield personnel from large radiation doses by mounting the target in a bunker behind a concrete curtain which can be drawn open or left closed when work has to be done in the area. Of course, most equipment is designed such that it rarely fails, but nevertheless interventions occur at least a few times a year.

The target is normally dumped into a waste-bin, hidden at the back of the bunker, before the shielding curtain is opened. In this way, and after a wait of 24 hours to let things cool down, the dose-rate in the zone amounts to between 20 to 24 mrem per hour.

Some simple remote handling devices are used to move targets and horns into and out of the bunker. During such operations, which can be carried out very quickly, the exposure rarely exceeds 100 mrem.

The downstream wall of the target-horn bunker is itself a collimator, also made of aluminium and cooled by demineralized water. A similar but somewhat larger arrangement which includes a steel core is used for dumping that part of the beam that escapes through the target bunker and does not contain the 3.5 GeV/c negatively charged particles directed into the AA.

5. SOME EXPERIMENTAL DEVICES FOR INCREASING THE $\bar{p}$-YIELD

Recently two experimental devices for increasing the $\bar{p}$ yield have been tested at the AA during machine development periods. Both are based on the wire lens principle. Neither are yet operational devices and so were dismounted after the experiments were completed.

The first device tested was a focusing target. Here 140 kA is pulsed through the 3 mm diameter, 88 mm long copper target attached to the front end of a magnetic horn. This is shown in Fig. 8.

The magnetic horn is focused on the end of the target. The $\bar{p}$ trajectories in the magnetic field inside the target (and just outside it) are essentially sinusoids, all particles with production angles less than some maximum value can be led to the end face of the target and more easily matched by the horn into the AA acceptance.

The latest of these devices so far tested gave an antiproton yield into the AA of 9×10^{-7} (to be compared with the normal value of 6×10^{-7}), but broke down after one hour's operation at half the normal repetition rate. During this last "durability" test, the high pressure nitrogen cooling system was exhausted and compressed air was used instead. This may have contributed to its breakdown because the cooling gas is led through very small grooves in the graphite close to the target where the temperatures may well be sufficient to rapidly oxidise the carbon.

The second device was a lithium lens fabricated by FNAL. This is illustrated in Fig. 9 and is described in detail by C. Hojvat et al.[9]. It is based on the pioneering work of B.F. Bayanov et al.[10] of Novosibirsk. This lens is 15 cm long and 2 cm in diameter and can sustain 500 kA of current in a pulse (half-sine) of 400 μs.

It is mounted as the primary of a 24 to 1 toroidal transformer and when tested, on a single shot basis, at the AA with a tungsten target gave a yield of 8.8×10^{-7} for p's. Mounted, as it is, directly after the target the transformer tends to get extremely radioactive. In normal operation at full AA duty cycle it is expected to give dose-rates of at least one thousand rem per hour, even more than the target.

The AA target area is not designed for remotely handling such a device but there are plans to do so because a combination of lithium lenses and pulsed focusing targets can enhance the AA $\bar{p}$-yield by up to a factor of two.

REFERENCES

1. C.D. Johnson, Antiproton Yield Optimization in the CERN Antiproton Accelerator, 1983 Particle Accelerator Conference, Santa Fe, New Mexico, CERN/PS/AA/83-11, 1983.

2. Summary of the Antiproton Collector Study, AA. Long Term Note 26, December 1983.

3. S. van der Meer, CERN Yellow Report 62-16.

4. E. Regenstreif, CERN Yellow Report 64-41.

5. G. Lebée, Corne AA, CERN/EP/81-03, 1981.

6. R. Bellone, G. del Torre, M. Ross, P. Sievers, The Design and Prototype Tests of the CERN Antiproton Production Target, CERN/SPS/80-9/ABT, 1980.

7. J. Ranft, H. Schönbacher, CERN-Lab. II-RA/TM/74-5, 1974.

8. E. Jones, S. van der Meer, F. Rohner, J.C. Schnuriger and T.R. Sherwood, Antiproton Production and Collection for the CERN Antiproton Accumulator, 1983 Particle Accelerator Conference, Santa Fe, 1983.

9. G. Dugan, C. Hojvat, A.J. Lennox, G. Biallas, F. Cilyo, M. Leininger, J. McCarthy, W. Sax and S. Snowdon, Mechanical and Electrical Design of the FNAL Lithium Lens and Transformer System, 1983 Particle Accelerator Conference, Santa Fe, New Mexico, 1983.

10. B.F. Bayonov, T.A. Vsevolozhskayer, Yu.N. Petrov and G.I. Silvestrov, The Investigation and Design Development of the Lithium Lenses with Large Operating Lithium Volume, 12th International Conference on High Energy Accelerators, FNAL, 1983.

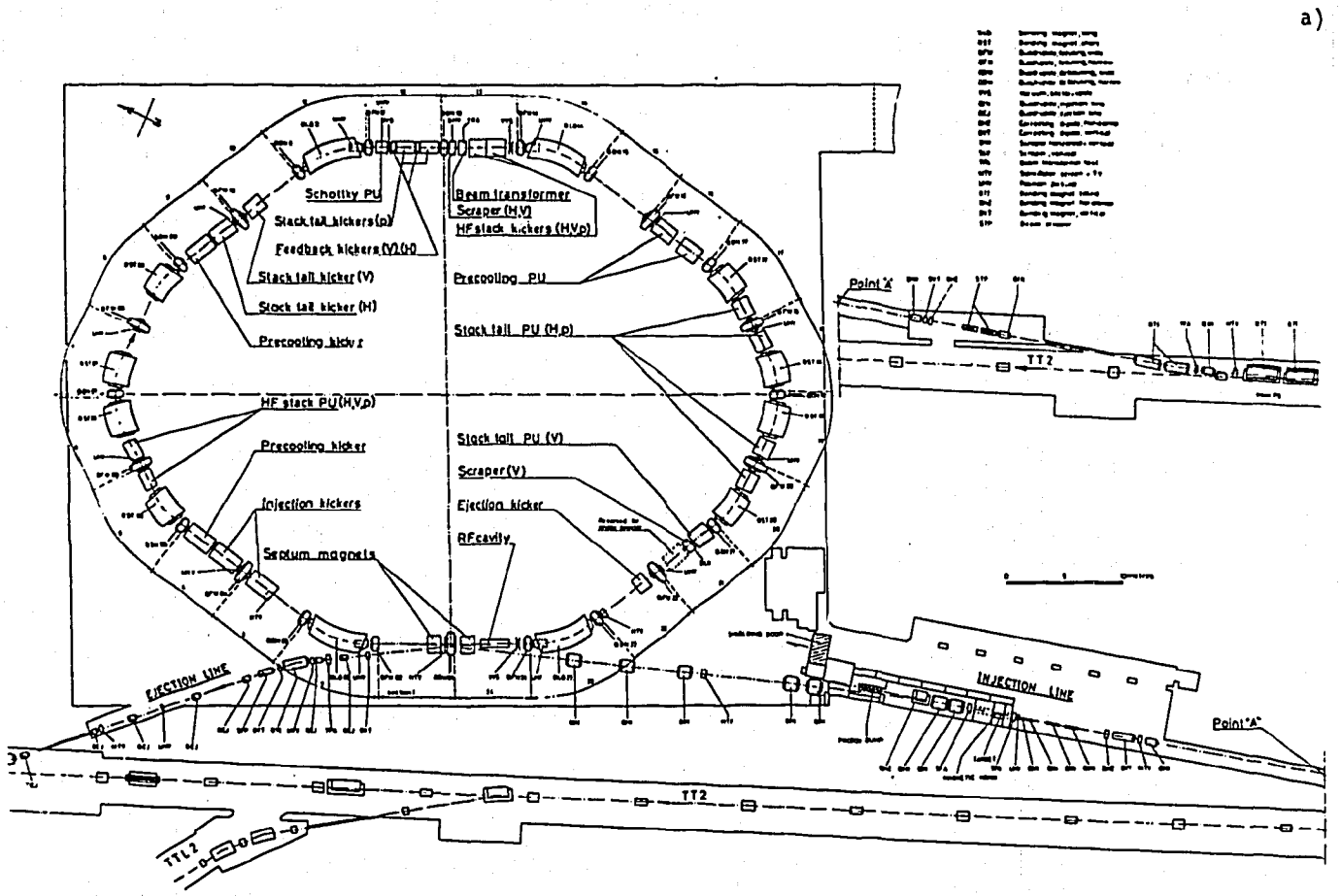

Fig. 1 a) Antiproton accumulator - General layout.
b) Target area to beam dump layout.

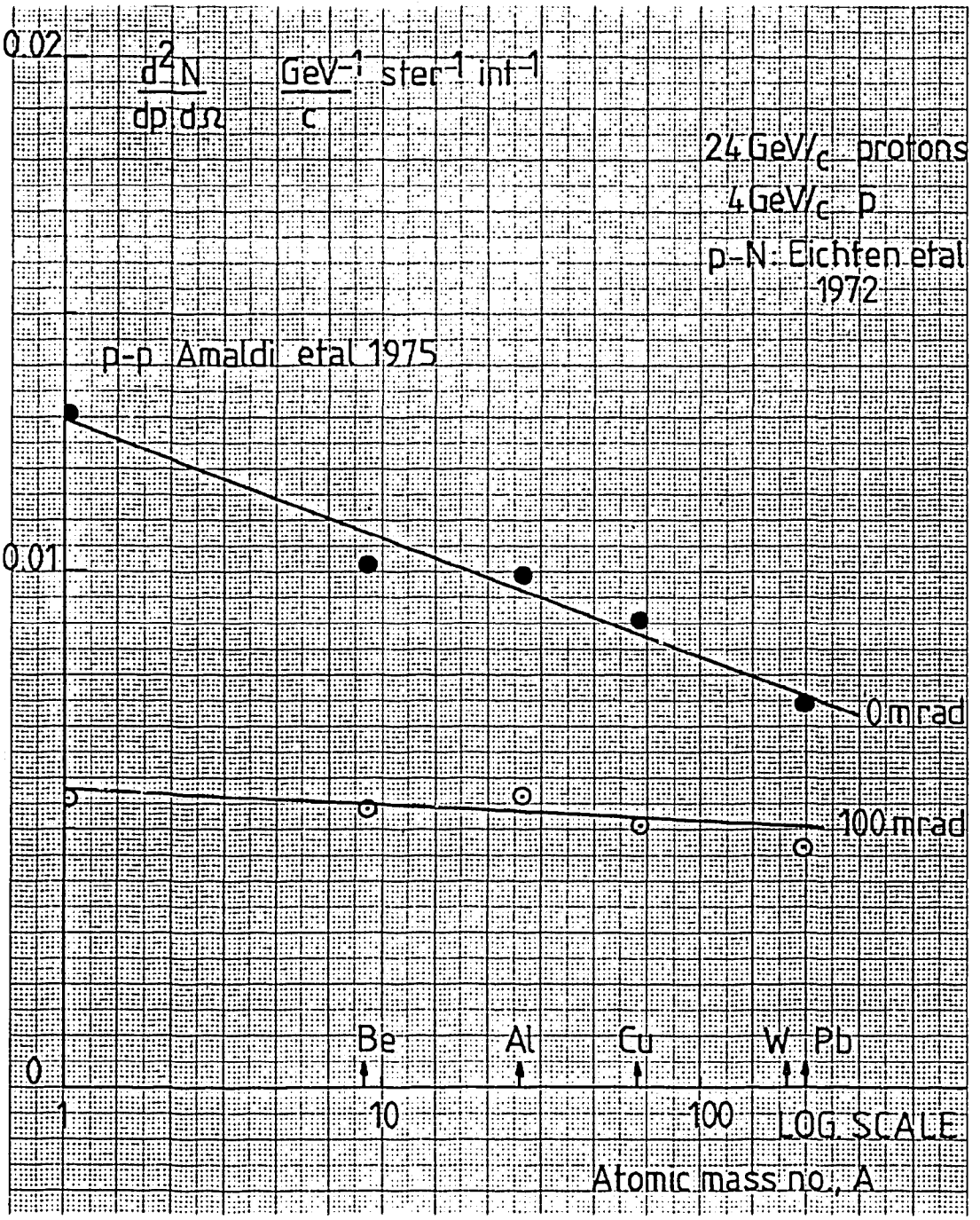

Fig. 2 $\bar{p}$ yield from pN collisions

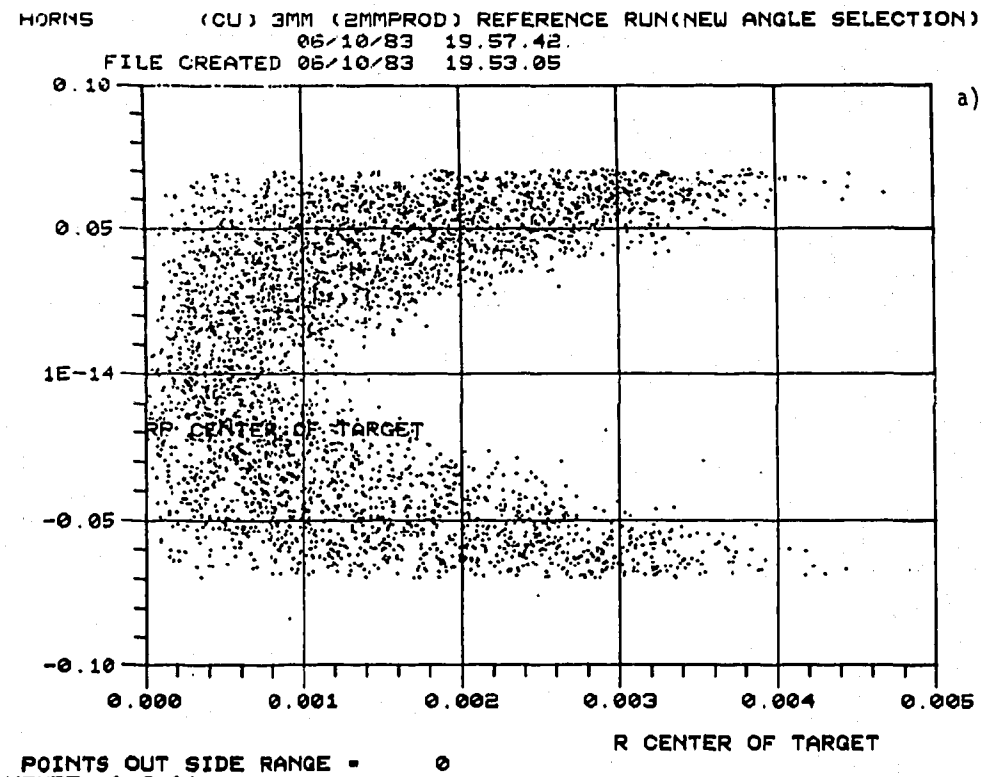

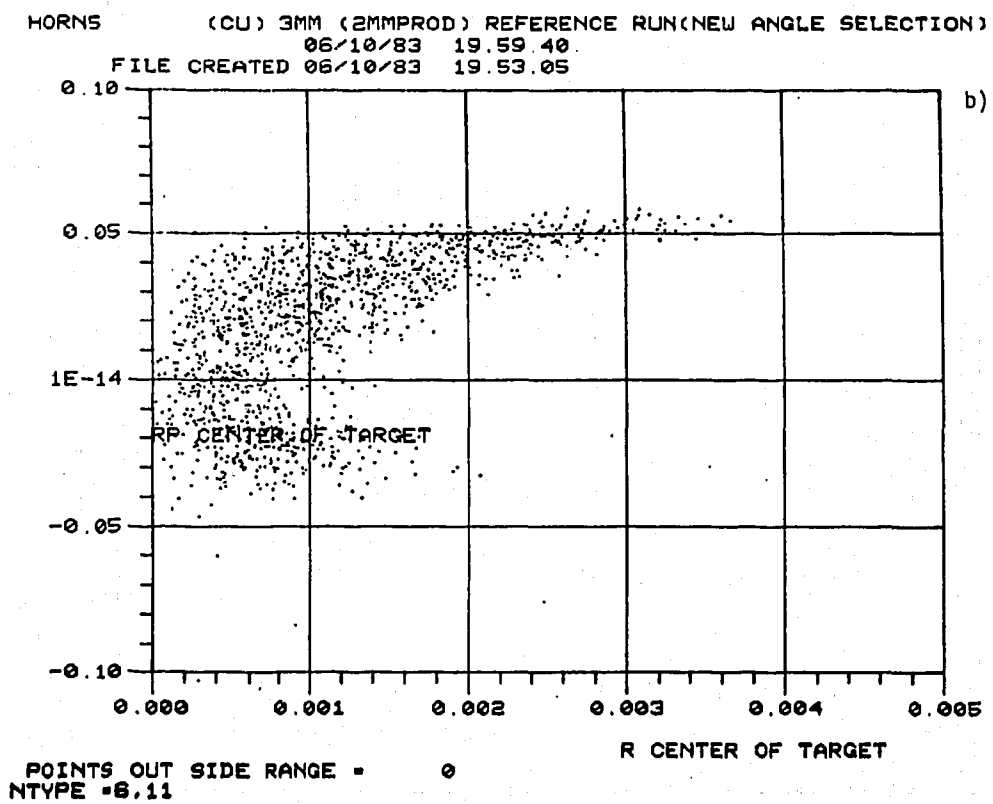

Fig. 3 a) Scatter graph of $\bar{p}$'s at centre of AA target.
b) $\bar{p}$'s at centre of target, but only those eventually matched to AA.

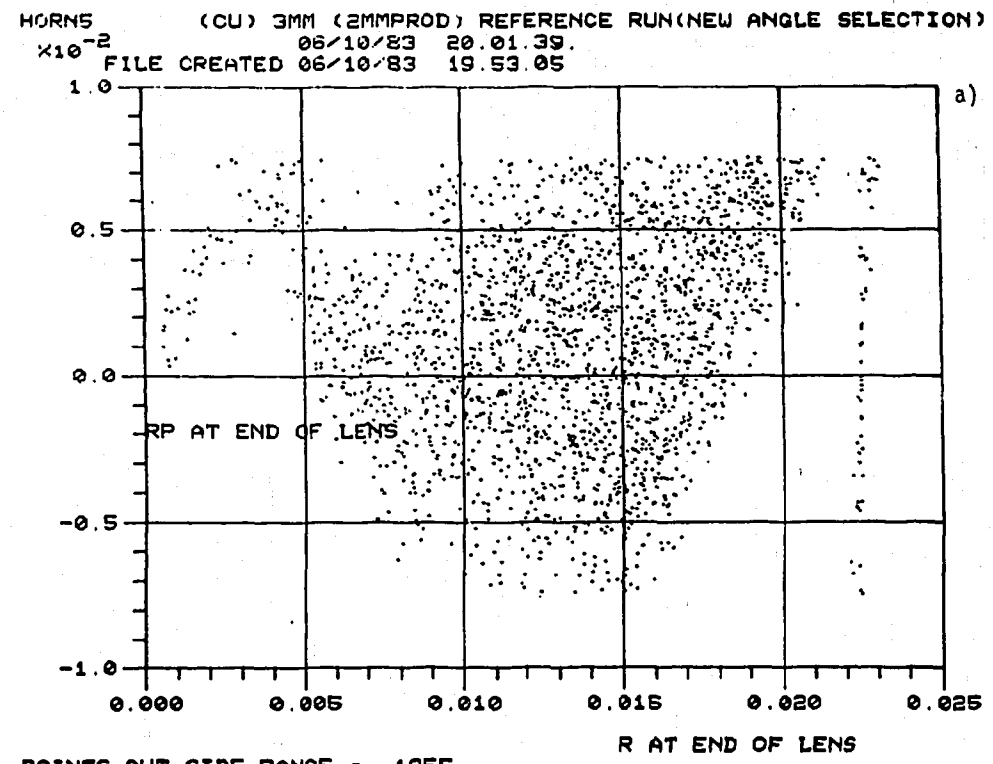

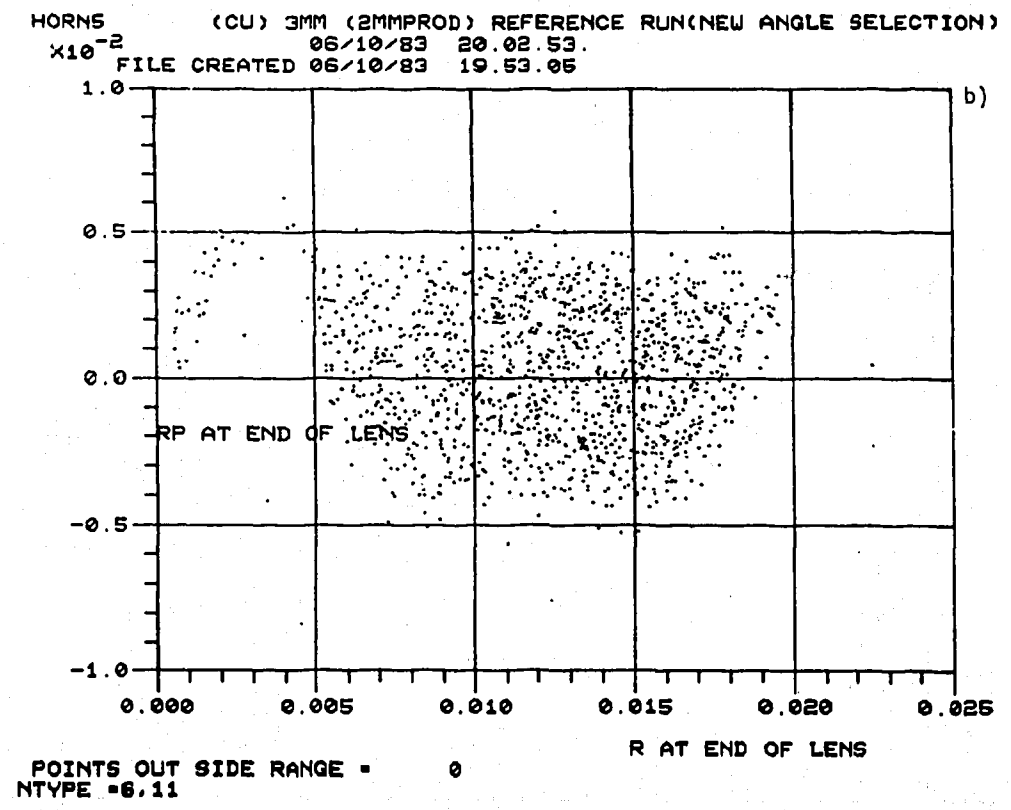

Fig. 4 a) Same $\bar{p}$'s as at target centre, but new at HORN exit.
b) Same $\bar{p}$'s as in (a) but only those captured into AA acceptance.

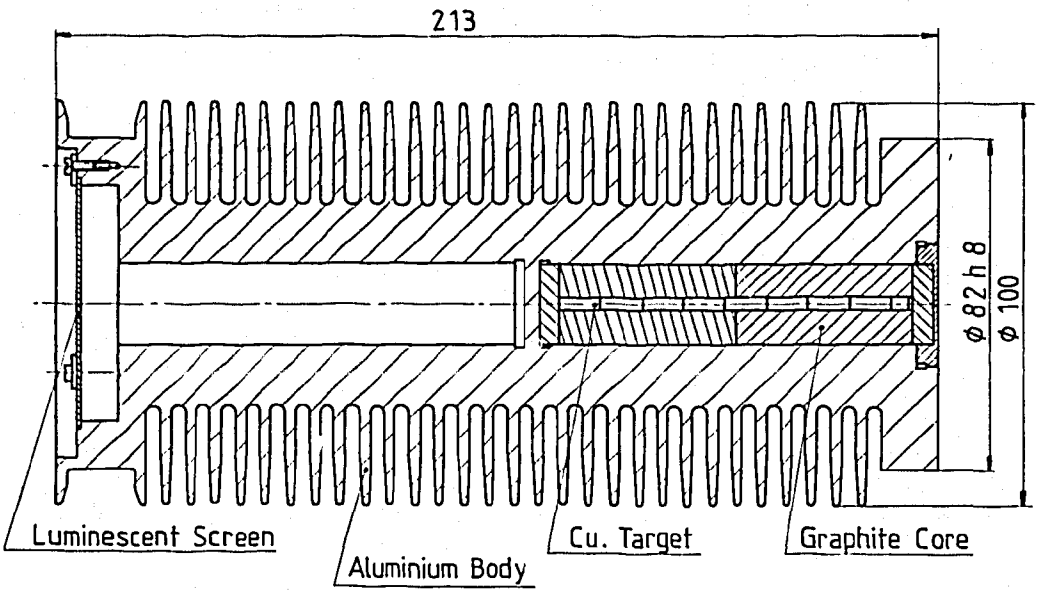

Fig. 5 Typical target assembly

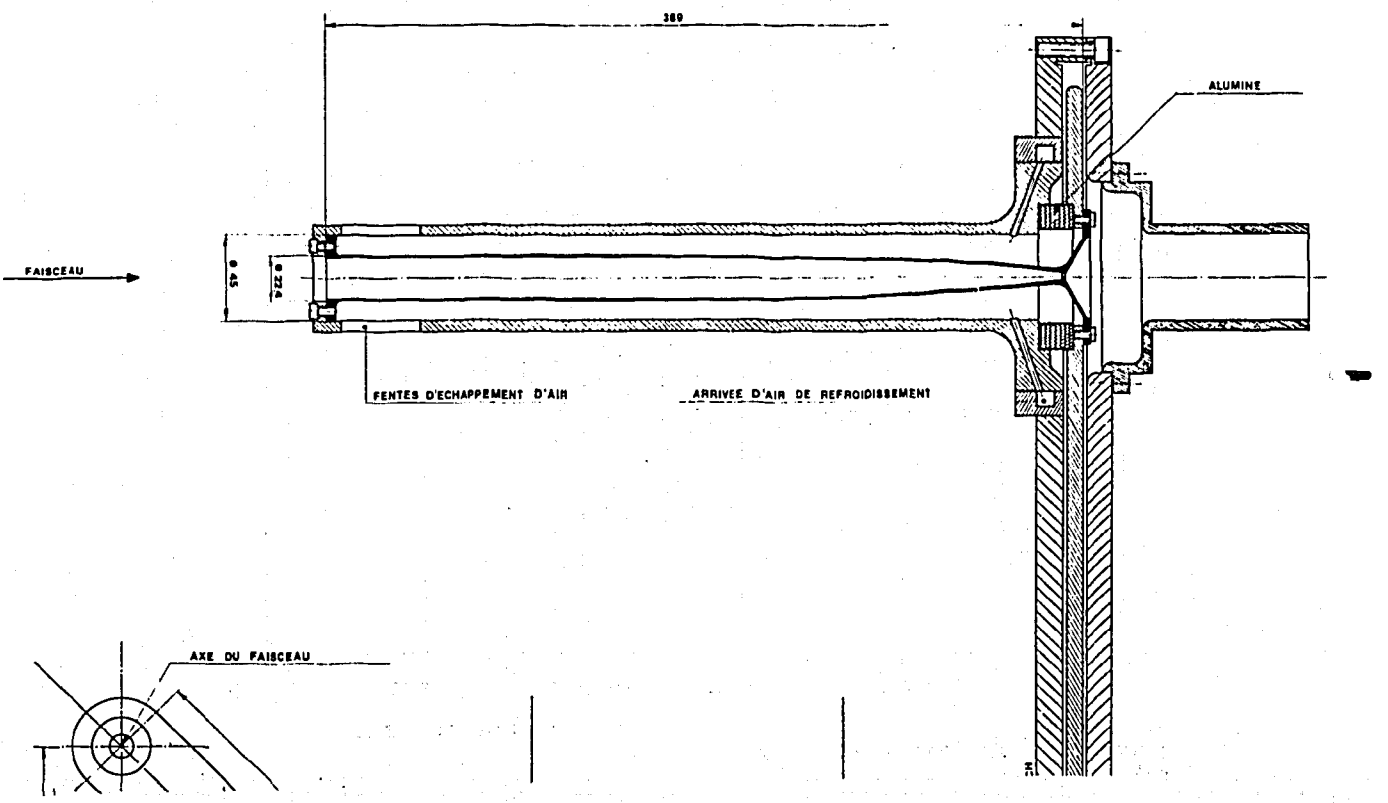

Fig. 6

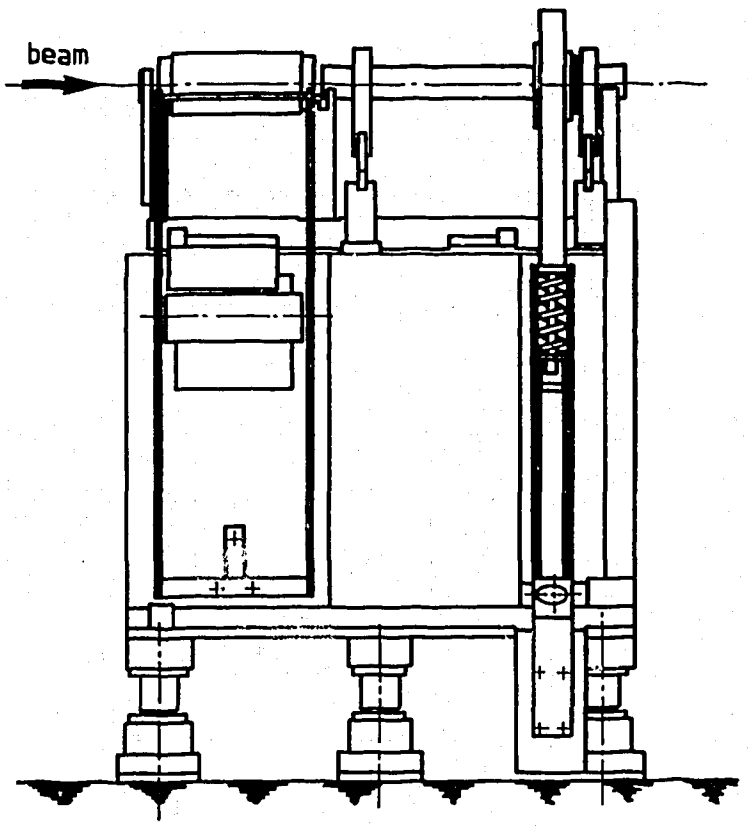

Fig. 7 Side view of horn and target assembly

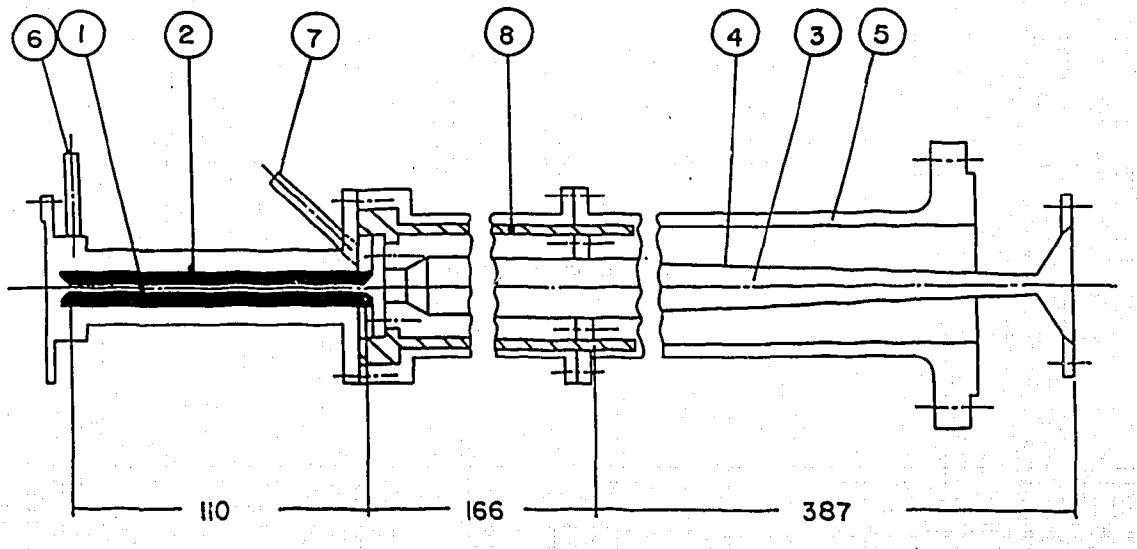

Fig. 8 Pulsed focusing target-horn. (1) is the copper target.

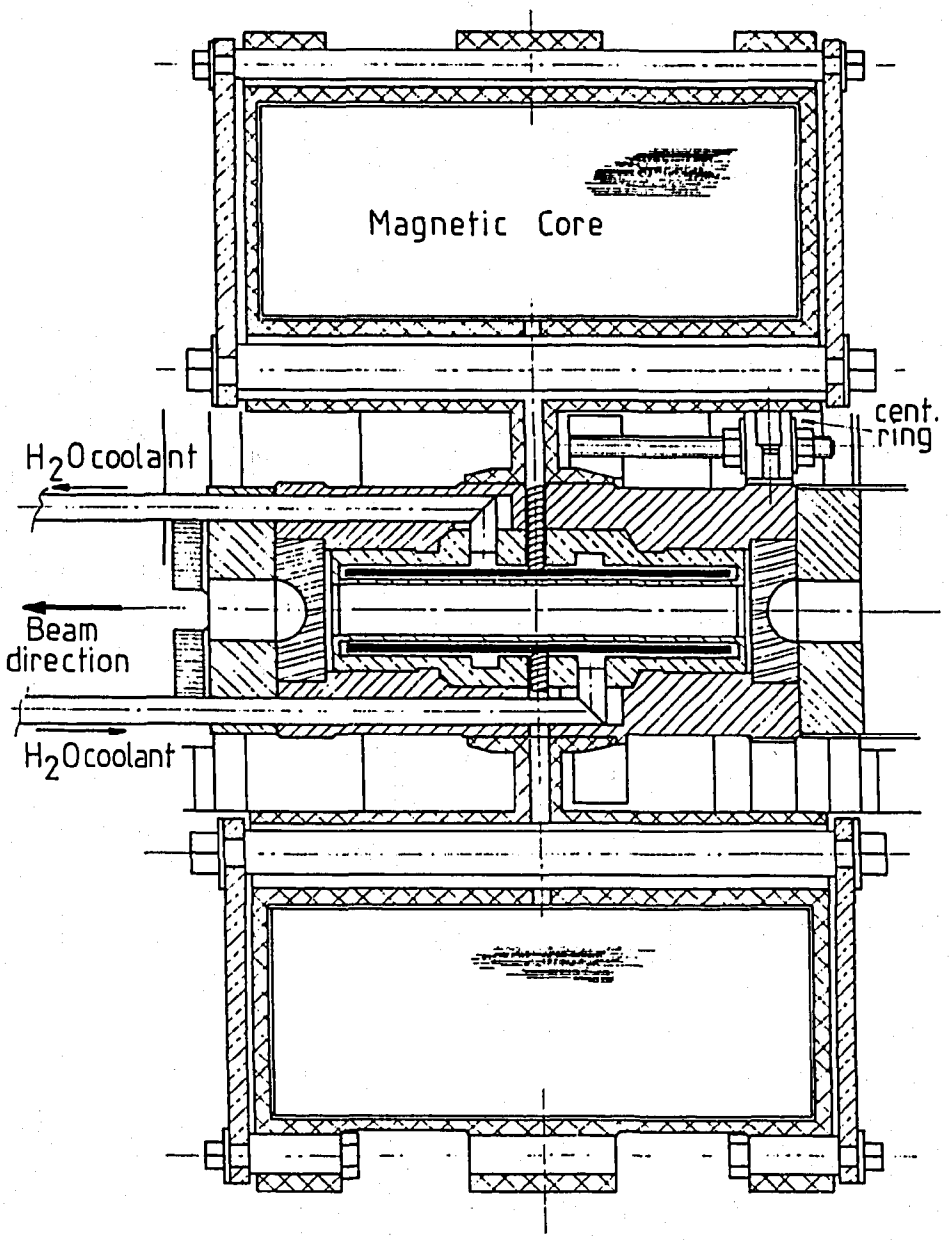

Fig. 9 FNAL lithium lens and transformer